scientific reports

Check for updates

OPEN

Synergistic effects of limestone calcined clay cement on alkalinity, mechanical performance, and vegetative compatibility of ecological concrete

Yi Fang[1]✉, Cheng Yang[2], Hui Zeng[3], Jin Yang[3], Hailong Zhang[3], Yue Gu[1], Hongqiang Chu[1]✉ & Linhua Jiang[1]

Ecological concrete is essential for sustainable construction, yet its application is limited by the high alkalinity of ordinary Portland cement (OPC), which inhibits plant growth, and by conventional alkalinity-reduction methods that often compromise mechanical performance. This study explores the use of limestone calcined clay cement (LC³) as a sustainable alternative, aiming to achieve a synergistic balance among low alkalinity, adequate compressive strength, and enhanced vegetative compatibility. LC³ ecological concretes with varying metakaolin and limestone contents and porosities of 22, 26, and 30% were prepared at a water-to-binder ratio of 0.24. The materials were characterized in terms of pH, compressive strength, hydration products (XRD, TGA/DTG, SEM, LF-NMR), pore structure, and plant growth performance using tall fescue over 60 days. Results indicate that LC³ significantly reduces 28-day pH to a plant-compatible range of 8.4–8.8, while mixes such as M20L15 and M30L15 achieve compressive strengths up to 13 MPa at 22% porosity. Microstructural analyses revealed that metakaolin's pozzolanic reaction consumes portlandite, and its synergy with limestone promotes the formation of dense C-A-S-H gels and carboaluminate phases, refining the pore structure and hindering alkali ion migration. Vegetation tests confirmed vigorous plant growth on LC³ concrete, particularly at 30% porosity, whereas OPC controls caused plant mortality. Overall, LC³ ecological concrete effectively addresses the limitations of conventional formulations, simultaneously ensuring mechanical integrity, controlling alkalinity, and supporting sustainable vegetative growth, highlighting its potential for green infrastructure applications.

Keywords Limestone calcined clay cement (LC³), Ecological concrete, Alkalinity reduction, Compressive strength, Vegetative compatibility

Ecological concrete has gained prominence in modern construction as a promising solution to meet the growing need for ecological restoration and sustainable urban development. Typically consisting of cement-bonded coarse aggregates with substantial porosity, this material can be applied in diverse settings such as urban rooftops, riverbanks, and slope surfaces[1]. By integrating a soil layer either above or within the concrete structure, grass and other vegetation can take root throughout the porous network. This promotes the ecological rehabilitation of built and natural surfaces while enhancing air quality and supporting broader environmental sustainability[2,3]. Given the escalating global focus on green infrastructure, ecological concrete holds considerable potential for mitigating the environmental footprint of conventional construction practices.

Despite these benefits, the widespread application of traditional ecological concrete is constrained by several critical challenges. The most prominent issue is its high alkalinity, which suppresses seed germination and plant growth, thereby undermining the long-term viability of vegetated systems[4–6]. The elevated pH within the pore

[1]College of Civil and Transportation Engineering, Hohai University, Nanjing 210098, People's Republic of China. [2]College of Material Science and Engineering, Hohai University, Nanjing 210098, People's Republic of China. [3]China Yangtze Power Co., Ltd, Yichang 443002, People's Republic of China. ✉email: yfang20@crimson.ua.edu; hhuchu411@126.com

Compositions	SiO_2	Al_2O_3	Fe_2O_3	CaO	MgO	SO_3	Na_2O
PC	14.61	8.47	5.30	66.27	1.41	1.70	1.03
CC	49.46	46.82	0.93	0.402	0.135	0.061	0.114
LS	0.698	0.58	0.39	97.65	0.42	0.025	/
GYP	0.024	0.028	/	47.178	/	52.69	/
SF	87.4	0.76	1.68	1.10	0.85	0.25	0.14

Table 1. Chemical compositions of Raw materials (mass fraction, %).

Aggregate size (mm)	Packed bulk density (kg/m^3)	Apparent density (kg/m^3)	Porosity (%)
10 ~ 20	1500	2700	45.6

Table 2. Basic performance indicators of gravel.

solution creates an unfavorable environment for most plant species, limiting the material's ability to achieve its intended ecological functions. This challenge highlights the urgent need for optimized formulations that balance mechanical performance with plant compatibility.

Current approaches to reduce alkalinity primarily include post-casting soaking treatments with acidic solutions and the use of low-alkalinity cements. While effective in lowering pH, these strategies present notable drawbacks. For example, sulfate-based soaking solutions may induce corrosion and long-term degradation of concrete[7–12], and the soaking process itself is impractical for large-scale or prefabricated elements. Similarly, low-alkalinity cements may compromise structural integrity and durability[13–16]. These limitations underscore the necessity of alternative binders capable of providing a more balanced performance.

Limestone Calcined Clay Cement (LC^3) has recently attracted attention as a potential solution for ecological concrete[17]. Compared with ordinary Portland cement, LC^3 offers several distinct advantages. At an appropriate water-to-cement ratio, the synergistic pozzolanic reaction between metakaolin and limestone promotes the formation of a denser microstructure, resulting in superior later-age strength[18–23]. The pozzolanic reaction of metakaolin, together with the filler effect of limestone powder and the densifying role of silica fume, work synergistically to significantly refine the concrete microstructure, thereby contributing to enhanced mechanical strength[24,25]. Previous studies further indicate that in LC^3, the pozzolanic reaction of calcined clay, combined with limestone-induced carboaluminate formation, promotes the formation of C-(A)-S-H gels and refines the pore structure. This microstructural refinement reduces pore connectivity and improves both resistance to chloride ingress and chloride-binding capacity. As a result, LC^3 concrete demonstrates superior durability under chloride exposure. Moreover, durability-based service life predictions and life-cycle assessments have shown that LC^3 systems can achieve longer projected service lives while substantially reducing carbon emission intensity on a per-service-year basis[26–28]. Owing to their sustained long-term pozzolanic activity, LC^3 systems also exhibit improved service life and durability compared to conventional concrete—a characteristic that is particularly advantageous for vegetated concrete applications[28–32]. However, current research on LC^3-based ecological concrete remains nascent, with the specific mechanisms governing its alkalinity regulation, pore structure evolution, and plant-compatibility still insufficiently understood.

Against this background, the present study provides a comprehensive evaluation of LC^3 for ecological concrete applications. Specifically, it investigates the effects of mix proportions and porosity on the alkaline environment and mechanical properties of LC^3-based ecological concrete. The mechanisms responsible for its reduced alkalinity are also elucidated. Furthermore, preliminary vegetation compatibility was assessed using tall fescue as a model species. By addressing the limitations of conventional ecological concrete and exploring LC^3 as a sustainable, low-alkalinity alternative, this research aims to deliver insights that facilitate the development of more durable, resilient, and eco-friendly construction materials.

Materials and methods

Materials and mixture design

The primary binder used was 42.5-grade ordinary Portland cement (PC), supplied by Wuhu Conch Cement Co., Ltd., with a specific surface area of 330 m^2/kg. Supplementary cementitious materials included ultra-high-reactivity metakaolin (MK, Inner Mongolia Chaopai), limestone powder (LS, 325 mesh, Henan Meishibo), and gypsum (GYP, dihydrate calcium sulfate, Xilong Chemical). A high-range water reducer (HRWR, Nanjing Subote) and silica fume (SF) were also incorporated. The chemical compositions of these raw materials are presented in Table 1. The coarse aggregate was gravel (10–20 mm), with a packed bulk density of 1500 kg/m^3, an apparent density of 2700 kg/m^3, and a porosity of 45.6% (Table 2).

The mix designs of the LC^3 blends are illustrated in Fig. 1. The control mix (Ctrl) contained 100% PC, while LC^3 formulations were produced by partially replacing PC with varying proportions of MK and LS, with GYP fixed at 5%. For instance, mix M20L15 consisted of 20% MK and 15% LS, replacing 40% of PC, whereas M30L10 contained 30% MK and 10% LS. This design matrix enabled a systematic evaluation of the combined effects of MK and LS on key performance indicators.

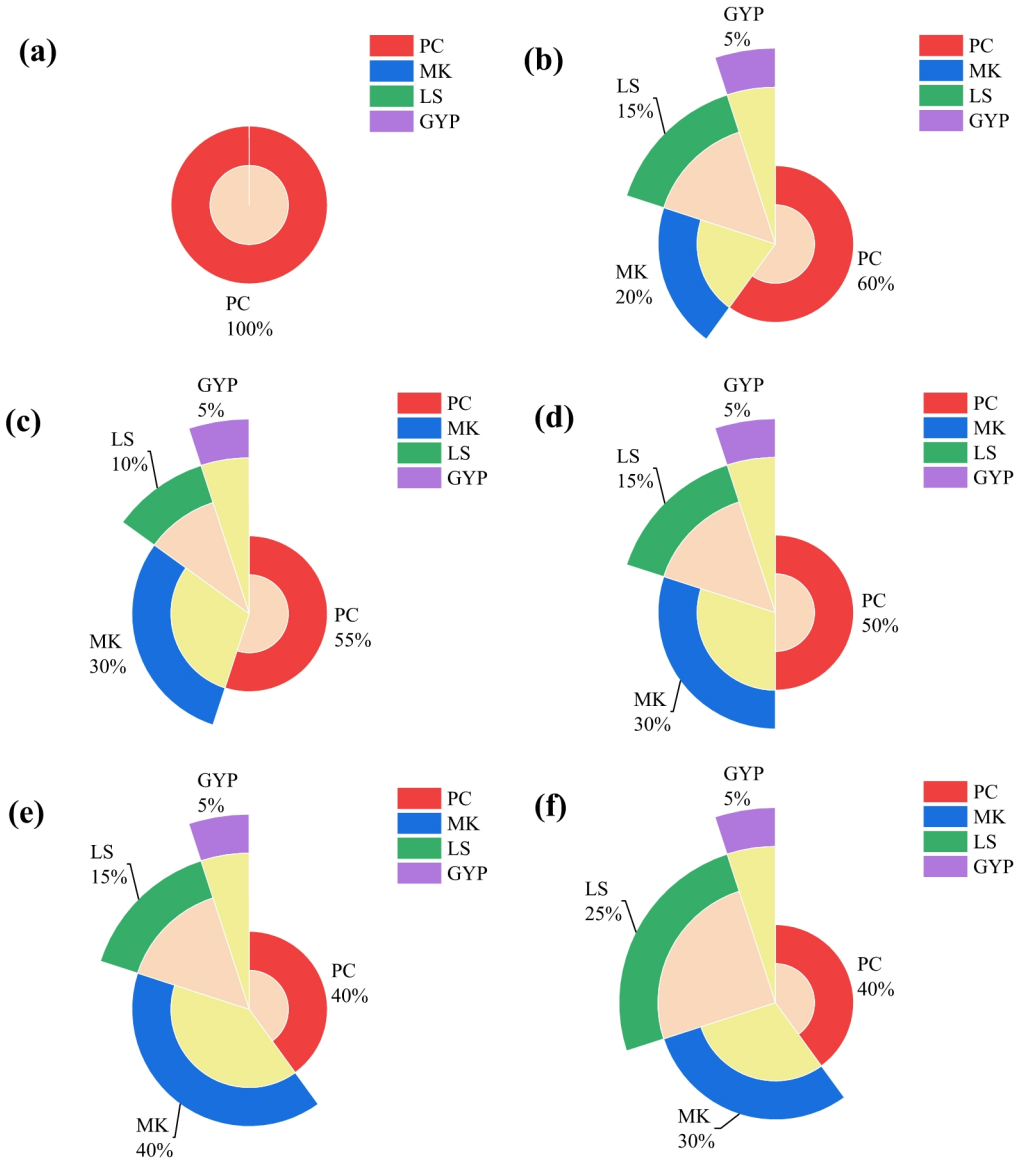

Fig. 1. Schematic diagram of LC^3 mix design: (**a**) Ctrl; (**b**) M20L15; (**c**) M30L10; (**d**) M30L15; (**e**) M40L15; (**f**) M30L25.

To ensure adequate mechanical performance of the vegetated concrete, priority was given to achieving a sufficiently high design strength of the cementitious matrix. Based on previous studies[33,34], a cement replacement level of approximately 60% has been reported to approach the upper limit beyond which strength deterioration becomes pronounced. Accordingly, six different LC^3 formulations were designed within this replacement range to maintain mechanical integrity. To balance plant growth with mechanical performance, three target porosities (22, 26, and 30%) were selected based on recommendations from previous studies[35,36]. The detailed mix proportions at a constant water-to-binder (w/b) ratio of 0.24 are summarized in Table 3.

Sample preparation and curing

The ecological concrete was prepared by first mixing binders, water, and additives into a homogeneous paste, followed by the addition of coarse aggregate, ensuring full coating. The fresh mixture was cast into molds in two equal layers, each compacted using a tamping rod and vibrating table. After 24 h, specimens were demolded and cured in a chamber at 20 ± 2 °C and > 95% relative humidity for 28 days. For comparison, LC^3 mortar specimens with the same binder composition and w/b ratio were also prepared and cured under identical conditions.

The designed porosity (P_{TP}), which is critical for root penetration, was calculated using Eq. (1):

$$P_{TP} = \left(1 - \frac{W_2 - W_1}{\rho V}\right) \times 100\% \quad (1)$$

Sample	PC	CC	LS	GYP	SF	Water	SP	Aggregate
Ctrl-22	304.4	/	/	/	6.1	74.1	1.6	1829.6
M20L15-22	179.4	59.9	44.9	15	6	73.3	6.1	1829.6
M30L15-22	147.9	88.74	44.4	14.8	5.9	72.4	6	1829.6
M40L15-22	118.4	118.4	44.4	14.8	5.9	72.5	12.7	1829.6
M30L10-22	166.4	90.7	30.3	15.1	6.1	74.1	6	1829.6
M30L25-22	119.7	89.8	40	15	6	73.2	9.5	1829.6
Ctrl-26	247.5	/	/	/	5	60.6	1.3	1829.6
M20L15-26	146	48.7	36.5	12.2	4.9	59.6	5	1829.6
M30L15-26	120.2	72.1	36.1	12	4.8	58.9	4.9	1829.6
M40L15-26	97.4	97.4	36.5	12.2	4.8	59.1	10.4	1829.6
M30L10-26	135.3	73.8	24.6	12.3	4.9	59	5	1829.6
M30L25-26	97.3	73	48.7	12.2	4.9	59.6	9	1829.6
Ctrl-30	190.4	/	/	/	3.8	46.6	1	1829.6
M20L15-30	113.9	38.2	28.7	9.6	3.8	46.6	3.9	1829.6
M30L15-30	92.6	56.7	28.3	9.4	3.7	45.8	3.8	1829.6
M40L15-30	75.9	75.9	28.4	9.5	3.7	46.4	8.1	1829.6
M30L10-30	105.9	57.8	19.3	9.6	3.8	47.1	3.9	1829.6
M30L25-30	76.4	57.3	47.8	9.6	3.8	46.8	7.4	1829.6

Table 3. Mix proportions of LC^3 ecological concrete (kg/m^3) with different porosities. PC = Portland cement, CC = Metakaolin, LS = Limestone Powder, GYP = Gypsum, SF = Silica fume, SP = Polycarboxylate Superplasticizer.

where W_1 is the saturated mass of the sample (after immersion in water), W_2 is the oven-dried mass (60 ± 2 °C for 24 h), V is the specimen volume, and ρ is the density of water. Cement paste specimens were $40 \times 40 \times 40$ mm^3, while concrete specimens were $150 \times 150 \times 150$ mm^3 cubes.

Vegetative growth experiment

Tall fescue, a cool-season grass, was selected as the test plant species due to its stable growth characteristics. The soil slurry was prepared by mixing horticultural soil (Sijihong Farm, Lianyungang) and nutrient soil (Miracle-Gro) at a 12:1 ratio, followed by the addition of water at a soil-to-water mass ratio of 0.6:1.

After 28 days of curing, the slurry was poured onto the concrete specimens and vibrated to ensure complete penetration into the pores, as illustrated in Fig. 2. Seeds were evenly broadcast on the surface and covered with 1–2 cm of nutrient soil. Germination was monitored every 24 h. Shoot height was measured every five days, beginning one week after germination and continuing until Day 30. Final shoot height and germination status were recorded at Day 60 to evaluate vegetation compatibility.

Test methods

Alkalinity

Two methods were utilized in this experiment to test alkalinity. First, for the ecological concrete, specimens were removed after 7 and 28 days of curing and placed in an appropriately sized container. Water was then added to achieve a solid-to-liquid ratio of 1:1, followed by a 24-hour waiting period. After calibrating the pH meter, the pH of the soaking solution was measured. The soaking solution was then drained and replaced with fresh water for another 24-hour interval, and the pH was measured again. This process was repeated until the difference between two consecutive pH measurements was within ±0.5. The second method was employed to test the alkalinity of LC^3 cement. After curing the cement for the same duration as the concrete, the cement was ground to a powder of approximately 0.15 mm. It was then mixed with water at a solid-to-liquid ratio of 1:4 and stirred thoroughly. Once the pH meter was calibrated, measurements of the solid-liquid mixture were taken until the pH readings stabilized.

Compressive strength

For the ecological concrete specimens measuring 150 mm × 150 mm × 150 mm and the LC^3 cement specimens measuring 40 mm × 40 mm × 40 mm, compressive strength tests were conducted after 28 days of curing. The compressive strength was evaluated in accordance with GB/T 50,081–2019.

XRD

X-ray diffraction (XRD) was performed on LC^3 ecological concrete to analyze its phase composition and determine the microstructural constituents. After 28 days of curing, the samples were crushed, collected, ground into powder, and dried. XRD testing was conducted using an Ultima IV X-ray diffractometer, covering a scanning angle range from 10° to 80° at a scanning speed of 5°/min.

Fig. 2. On-site seeding of ecological concrete specimens after 28 days of curing.

Pulse sequence	TD	SW	RFD	RG1	DRG1	PRG	TW	NS	NECH	TE	DL1
FID	1024	100	0.02	20	3	2	2000	4	/	/	/
CPMG	auto	200	0.02	10	3	2	1000	32	2000	0.11	500

Table 4. Values for basic parameters of LF-NMR instrument.

TGA

Thermogravimetric analysis (TGA) was employed to supplement the verification of mineral phase composition in LC_3-based cement pastes. The powdered samples were subjected to a temperature ramp from 30 °C to 1000 °C under a nitrogen atmosphere, with a constant heating rate of 10 °C/min.

SEM

SEM analysis was performed using a Zeiss scanning electron microscope on concrete slices extracted from 28-day-cured specimens. Prior to imaging, the samples were dried, dehydrated, and fixed to ensure microstructural clarity.

NMR

Low-field nuclear magnetic resonance (LF-NMR) measurements were performed using a PQ001 analyzer (Niumag, Suzhou, China), with a magnetic field strength of 0.42 T and a resonance frequency of 18 MHz. During testing, the magnet temperature was controlled at 32 ± 0.02 °C, and the ambient laboratory temperature was maintained at 20 ± 2 °C.

The transverse relaxation time T_2 was measured using the Can-Purcell-Meiboom-Gill (CPMG) pulse sequence. Prior to testing, instrument calibration was carried out with a Free Induction Decay (FID) sequence using a standard oil reference. The acquisition parameters are listed in Table 4. All samples were tested under full saturation conditions. The resulting T_2 distribution was used to analyze pore structure and pore volume distribution, and the integrated signal area was used to calculate the total porosity.

Results and discussions

Physical performance of LC³ ecological concrete

Compressive strength

Figure 3 shows the 28-day compressive strength of LC³ ecological concrete as a function of mix proportion and porosity at a constant water-to-binder ratio of 0.24. The results indicate substantial variations among the different formulations. Mixes M20L15, M30L15, and M30L10 exhibited higher compressive strength than the control (100% PC) at all porosity levels, whereas M40L15 and M30L25 consistently showed lower strength. For example, at 22% porosity, M20L15 achieved a strength of approximately 13 MPa, representing a 37.5% increase over the control (9.5 MPa). In contrast, M40L15 reached only about 9.1 MPa, 4.2% lower than the control.

The reduced performance of M40L15 and M30L25 can be attributed to their high clinker replacement level (60%). Excessive metakaolin content may delay strength development at early ages, while the large proportion of limestone introduces a dilution effect, producing a less compact microstructure compared with ordinary Portland cement paste. These findings suggest that beyond a certain threshold, the benefits of the metakaolin–limestone synergy are outweighed by the reduction in clinker content, resulting in diminished strength. Previous studies have demonstrated that, with appropriate mix design, LC³ cementitious matrices can achieve relatively high strength levels[33], a finding that is also corroborated by the results presented in this study. However, excessively high cement replacement ratios may introduce adverse effects that reduce matrix strength below that of conventional Portland cement–based designs.

The mechanical performance of vegetated concrete is governed primarily by two factors. As discussed above, the first is the strength of the cementitious matrix; the second concerns the formation and characteristics of the pore structure, which becomes the focus of the following discussion. A strong negative correlation between porosity and strength was observed. As porosity increased from 22% to 30%, the compressive strength of all mixes declined markedly. For instance, M20L15 decreased from 13 MPa to about 7 MPa, a reduction of 46.2%. The distinctive layered structure of metakaolin can significantly influence the rheological behavior of cementitious systems, leading to an increase in viscosity[37]. As a result, LC³-based binders tend to achieve denser aggregate bonding than ordinary Portland cement, particularly at lower porosity levels, where strength enhancement becomes more pronounced. Conversely, higher porosity reduces the amount of cementitious material available for effective aggregate bonding and is further compounded by diminished workability[38], resulting in a more evident decline in mechanical strength. Overall, the LC³-based vegetated concrete achieved the required compressive strength of 9 MPa specified by JC/T 2557 – 2020 at a porosity of 22%, while also exhibiting improved performance compared with conventional Portland cement–based vegetated concrete. Consequently, precise control of porosity is essential to achieving a balance between the ecological requirement for root penetration and the mechanical performance of LC³ ecological concrete.

Alkalinity

The initial pH values of the ecological concrete at 7 days are shown in Fig. 4. Although the pH of LC³-based mixes is generally lower than that of the control, it remains in the range of 10.6–10.9, which is still well above the target pH of 9 considered suitable for plant growth. This suggests that even with substantial clinker replacement, the limited calcium hydroxide (CH) generated during hydration is sufficient to maintain a strongly alkaline environment.

At identical water-to-binder ratios and porosity levels, the variation in pH among the LC³ mixes is relatively small but still discernible. Mixes with higher OPC contents, such as M20L15 and M30L15, consistently exhibit higher pH values, often exceeding 11. By contrast, mixes with greater clinker replacement, such as M40L15 and M30L25, display slightly lower pH, in some cases falling below 11. This difference can be attributed to the higher residual CH content in OPC-rich mixes, while in high-metakaolin and limestone blends, pozzolanic and carboaluminate-forming reactions consume more CH, thereby reducing alkalinity.

A notable decrease in pH occurs between 7 and 28 days of curing. Mixes with higher OPC content (e.g., M20L15, M30L10) maintain relatively elevated pH levels throughout this period, whereas those with high metakaolin and limestone contents (e.g., M40L15) show a more pronounced decline. This trend is primarily

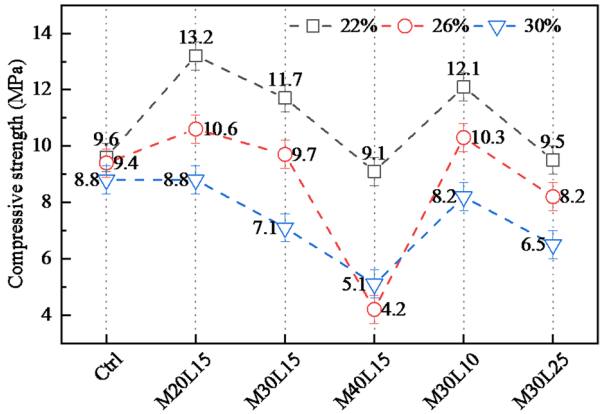

Fig. 3. Compressive strength of LC³ ecological concrete at 28 days.

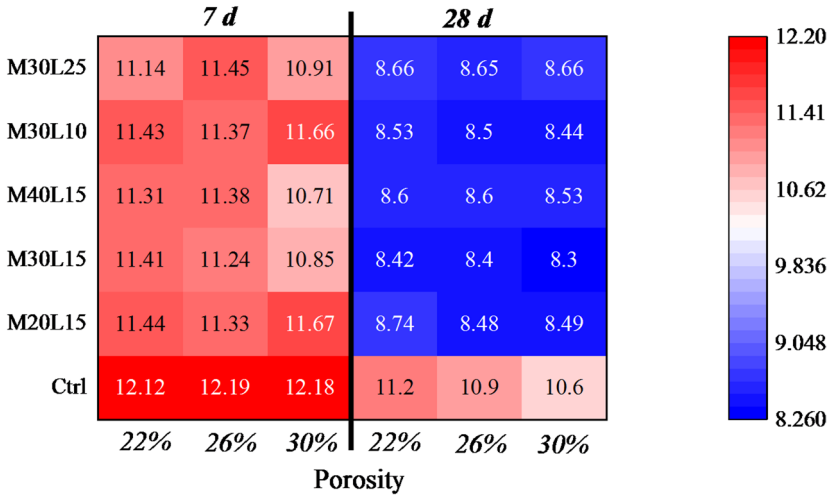

Fig. 4. pH of LC^3 ecological concrete at different curing ages.

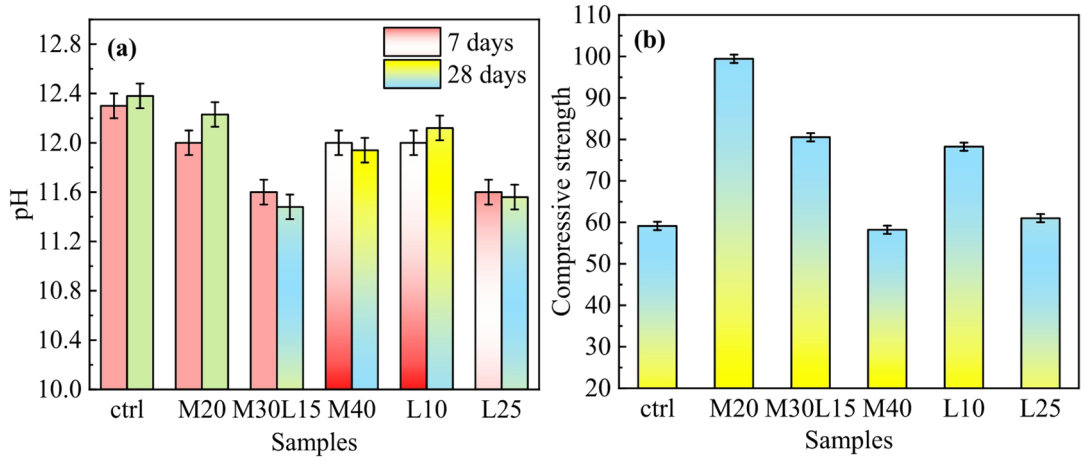

Fig. 5. Physical properties of LC^3 pastes specimens: (**a**) pH; (**b**) compressive strength.

driven by the continuous pozzolanic reactions, which progressively consume CH. At the same time, these reactions refine the microstructure, reducing pore connectivity and limiting the leaching of alkaline ions, which indirectly lowers the measurable pH.

In addition, we consider the compactness of the cementitious matrix to play a critical role in the performance of LC^3 specimens. Previous studies have shown that controlling the surface densification of vegetated concrete can effectively suppress the leaching of alkaline ions[39,40]. LC^3 binders inherently exhibit a high degree of matrix densification[23,41], a characteristic that is further corroborated by the SEM observations presented later in this study. Owing to the synergistic interaction between pozzolanic reactions and limestone-related effects, the overall compactness of LC^3-based vegetated concrete is substantially enhanced, which in turn markedly restricts alkali release and contributes to the observed reduction in alkalinity. This interpretation is consistent with the results obtained from the cementitious matrix tests discussed subsequently.

Overall, the results at both 7 and 28 days indicate that alkalinity is governed primarily by the degree of OPC replacement and the associated consumption of CH through pozzolanic reactions. Early-age high pH values are controlled by initial hydration releasing hydroxide ions, whereas the subsequent decline reflects the gradual depletion of CH. From an ecological perspective, LC^3-based ecological concrete with a water-to-binder ratio of 0.24 exhibits the potential to develop a more plant-compatible alkaline environment over time. Its alkalinity remains below the maximum pH threshold of 9 specified in JC/T 2557 – 2020 for vegetated concrete systems, with the M40L15 mixture showing the greatest potential for further alkalinity reduction.

Relationship between alkalinity and compressive strength

To elucidate the interplay between alkalinity and compressive strength in LC^3 ecological concrete, cement pastes were tested at a water-to-binder ratio of 0.24. As shown in Fig. 5(a), the pH values of LC^3 pastes, although generally above 11.0 at both 7 and 28 days, are consistently lower than that of the pure OPC control. The control

paste maintained a high pH of approximately 12.6 at 7 days, decreasing only slightly to 12.3 at 28 days. In contrast, all LC³ mixes exhibited a more pronounced pH reduction over time, primarily due to the pozzolanic reaction of metakaolin, which consumes calcium hydroxide (CH), and the influence of limestone on the crystallization of hydrate assemblages. Despite this reduction, the pH of LC³ systems remains sufficiently high to ensure a durable alkaline environment.

Figure 5(b) highlights a clear variation in compressive strength among the formulations. Mix M20L15 achieved the highest strength, approaching or exceeding 99 MPa, demonstrating the exceptional mechanical performance attainable with an optimized LC³ proportion. However, as the replacement level of metakaolin and limestone increases (e.g., in M40L15 and M30L25), compressive strength decreases noticeably. This decline is mainly due to reduced clinker content, which limits the primary formation of strength-contributing C–S–H and CH. Nevertheless, a moderate metakaolin content promotes additional C–S–H formation through secondary pozzolanic reactions, while the interaction between limestone and metakaolin facilitates the formation of monocarboaluminate, enhancing microstructural density and partially compensating for strength loss.

Importantly, the results indicate that pH and compressive strength are not directly correlated. Although the control sample exhibits the highest pH, its strength is surpassed by several LC³ mixes. Mechanical properties are governed not solely by CH content but, more critically, by the quantity of C–(A)–S–H gel and overall microstructural density. This observation aligns with literature suggesting that even a small amount of CH is sufficient to maintain high alkalinity[42]. The pozzolanic reaction of metakaolin consumes CH while simultaneously producing additional C–(A)–S–H gels, resulting in a denser matrix that enhances strength and inhibits ion transport[43].

In ecological concrete, alkalinity leaching is primarily controlled by ion transport through the pore network[4,44]. While surface treatments (e.g., paraffin coatings) can temporarily impede ion migration, the ongoing pozzolanic reactions in LC³ systems promote continuous microstructural refinement over time[27,45]. This gradual densification effectively suppresses the leaching of alkaline ions, providing a more sustainable means to maintain a plant-compatible environment without compromising long-term mechanical performance.

Hydration products

XRD analysis

The XRD patterns of the control (Ctrl) and LC³ samples with a w/b ratio of 0.24 after 28 days of hydration are shown in Fig. 6, highlighting the evolution of mineralogical phases with varying binder compositions. The Ctrl sample exhibits distinct diffraction peaks for portlandite (CH) at approximately 18.1° and 34.1°, reflecting a substantial presence of $Ca(OH)_2$, the primary contributor to the high alkalinity in ordinary Portland cement systems. By contrast, LC³ samples display progressively weaker CH peaks with increasing metakaolin and limestone content. In particular, the CH reflections are nearly absent in M40L15, indicating extensive CH consumption through pozzolanic reactions—consistent with the marked reduction in alkalinity observed in these mixes.

Simultaneously, the intensity of the calcite ($CaCO_3$) peak near 29.4° increases within the LC³ series, especially in M30L25. This can be attributed to: (1) the direct incorporation of limestone powder, which may remain partially unreacted due to limited reactivity, and (2) carbonation of residual CH during curing or specimen preparation, further lowering alkaline species and potentially contributing to surface densification[46]. Quartz peaks are present in all mixes, derived from inert raw material phases, and remain largely unchanged, confirming its limited role in hydration. LC³ samples also exhibit ettringite (AFt) peaks, though under high metakaolin content the available aluminum is more likely incorporated into C–A–S–H gels or carboaluminate phases rather than forming large quantities of AFt. The presence of limestone further facilitates carboaluminate formation and can stabilize AFt against decomposition[47,48]. Residual belite (C_2S) peaks persist across all specimens, suggesting

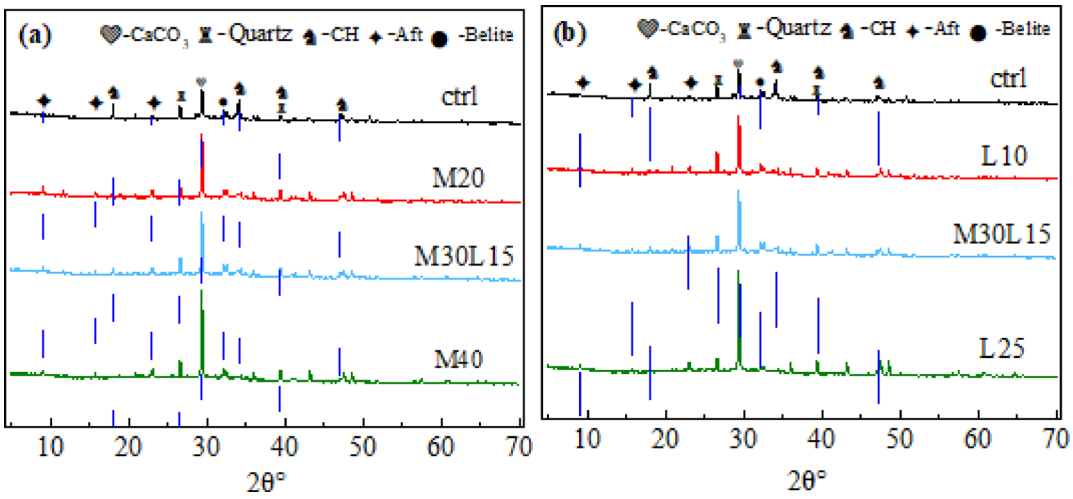

Fig. 6. XRD patterns of samples after 28 days of hydration.

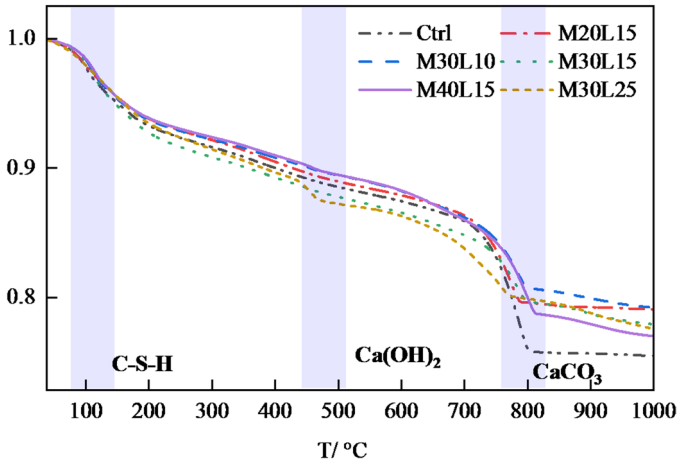

Fig. 7. TG curves of samples with different binder compositions at 28 days.

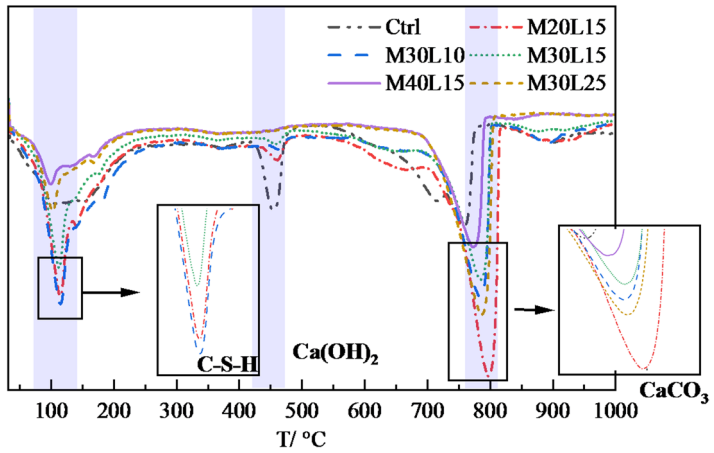

Fig. 8. DTG curves of samples with different binder compositions at 28 days.

unhydrated clinker remains and that continued hydration could contribute to further long-term strength development.

Overall, the XRD results demonstrate that LC³ systems effectively consume portlandite, thereby reducing alkalinity while promoting the formation of carboaluminates and other secondary hydrates. These mineralogical changes align with the observed pH reductions and microstructural refinement, supporting LC³ as a viable binder for ecological concrete applications.

TGA analysis

Thermogravimetric analysis (TGA) and derivative thermogravimetry (DTG) were performed on LC³ mixtures after 28 days of curing at a w/b ratio of 0.24 to quantify hydration products. The results are presented in Fig. 7 (TGA) and Fig. 8 (DTG), with the analysis focusing on three key temperature regions.

The first mass loss, observed between 100 and 200 °C, is primarily associated with the dehydration of C–S–H gel and ettringite (AFt). All mixtures exhibited notable weight loss in this region, with M20L15 and M30L10 showing steeper curves. This indicates a higher bound water content, suggesting greater degrees of hydration and C–S–H formation[49,50]. Between 400 and 550 °C, the mass loss corresponds to the dehydroxylation of portlandite ($Ca(OH)_2$). The Ctrl sample exhibited a sharp decline, reflecting substantial CH generation from OPC hydration. In contrast, the LC³ mixtures displayed markedly lower mass losses, with M40L15 showing the smallest peak. This trend highlights the effective consumption of CH by the pozzolanic reaction of metakaolin, resulting in reduced residual CH content compared with the control. In the 650–800 °C range, the mass loss is attributed to the decomposition of calcium carbonate ($CaCO_3$). While negligible in the Ctrl sample, distinct peaks were observed in the LC³ mixtures, particularly in M30L15 and M30L25. The intensity of this peak increased with limestone dosage, as expected.

The DTG curves (Fig. 8) corroborate these findings. The peak around 150 °C, corresponding to C–S–H dehydration, was most prominent in M20L15 and M30L10, consistent with TGA observations. The decomposition temperature (~ 140–150 °C) was similar across all mixes, suggesting comparable decomposition mechanisms[33].

The $Ca(OH)_2$ peak near 450 °C was strong in the Ctrl sample but significantly reduced in the LC^3 mixes, while the $CaCO_3$ peak at ~ 750 °C was negligible in Ctrl yet pronounced in the LC^3 samples, with intensity scaling with limestone content.

Together with the XRD results, the TGA/DTG analysis confirms that the reduced alkalinity of LC^3 systems is primarily linked to the pozzolanic consumption of portlandite. Although a small amount of residual CH remains—sufficient to sustain high pH for ongoing hydration and durability—the overall reduction contributes to a more plant-compatible alkaline environment.

SEM

Figure 9 presents the SEM micrographs of LC^3 mortar specimens after 28 days of curing, highlighting significant differences in microstructural development across the mix designs. The control sample (Ctrl, Fig. 9a), composed solely of OPC, exhibits a relatively loose and discontinuous matrix. Scattered unhydrated cement particles, microcracks, and a limited amount of hydration products (e.g., C–S–H) are evident, consistent with its lower compressive strength and compactness.

The incorporation of metakaolin (MK) and limestone (LS) significantly improves the matrix structure. In M20L15 (Fig. 9b), the matrix is visibly denser, with fibrous and gel-like hydration products, mainly C–S–H and alumina-rich C–A–S–H phases, more uniformly distributed. This indicates that the pozzolanic reaction of MK refines the pore structure and enhances particle bonding. A more extensive and compact gel matrix is observed in M30L10 (Fig. 9e), which contains higher MK content. The surface is covered with overlapping fibrous structures and needle-like hydrates, suggesting a more complete reaction. The reduction in visible pores and cracks reflects improved matrix integrity, which corresponds to its higher compressive strength.

The most optimized microstructure is found in M30L15 (Fig. 9c). Hydration products are abundant and uniformly distributed, with minimal voids. This indicates an effective synergy between MK and LS at this ratio, promoting the formation of both C–A–S–H gels and carboaluminate phases (e.g., hemi- and monocarboaluminate). These phases effectively fill pores, strengthen the interfacial transition zone, and result in a continuous, compact, and homogeneous matrix. By contrast, further increasing MK content to 40% (M40L15, Fig. 9d) leads to microstructural deterioration. Although abundant hydrates are formed, local agglomeration and uneven gel distribution are apparent. The presence of unreacted MK clusters suggests that the w/b ratio may be insufficient for complete reaction at this replacement level, producing micro-voids and reducing homogeneity. Similarly, excessive LS content (25% in M30L25, Fig. 9f) results in a looser matrix compared with M30L15. While LS facilitates nucleation, excessive dosage dilutes reactive phases, limiting gel continuity. This leads to a fragmented matrix with higher porosity, consistent with its lower mechanical strength.

In summary, SEM analysis confirms that moderate MK and LS replacements (e.g., M30L15) significantly densify the microstructure of LC^3 ecological concrete by promoting cohesive hydration products, whereas excessive SCM content causes incomplete reactions or dilution effects, thereby weakening the matrix. These microstructural findings are in strong agreement with the observed trends in compressive strength and alkalinity.

Pore structure via LF-NMR analysis

The pore size distributions of the control and LC^3 pastes, determined by low-field nuclear magnetic resonance (LF-NMR), are shown in Fig. 10. All samples exhibit a bimodal distribution, with the first peak between 1 and 10 nm corresponding to gel pores, and the second, more pronounced peak between 100 and 1000 nm corresponding to capillary pores.

The control sample displays the highest overall pore volume, particularly in the capillary range, reflecting a relatively loose microstructure with a high volume of interconnected large pores. In contrast, all LC^3 blends exhibit a significant refinement of the pore structure. The second peak is markedly reduced or absent, indicating a shift toward a finer, gel-dominated pore system.

The degree of refinement varies with mix design. The most substantial reduction in capillary porosity occurs in M20L15, followed by M30L10 and M30L15. This trend correlates with their higher compressive strengths and is attributed to the effective pozzolanic reaction of metakaolin and the synergistic role of limestone. At clinker replacement levels below 50%, sufficient $Ca(OH)_2$ is available to react with metakaolin, forming dense C–A–S–H gels and carboaluminate phases that effectively fill capillary pores. Mixtures such as M30L25 and M40L15 exhibit gel pore volumes comparable to the control, yet their capillary porosity is markedly lower. This indicates that even with a limited quantity of hydration products, the connectivity of the large-pore network is effectively disrupted.

This pore structure refinement is critical in explaining the reduced alkalinity of LC^3 ecological concrete. Alkalinity leaching primarily depends on ion transport through capillary pores[51,52]. Therefore, the reduced volume and connectivity of capillary pores in LC^3 systems significantly hinder ion migration, complementing the chemical consumption of $Ca(OH)_2$. In effect, LC^3 not only reduces the source of alkalinity but also limits its transport, achieving a similar protective mechanism to surface sealers (e.g., silane-based treatments) that penetrate and block capillary pores to inhibit leaching[53–55].

Total porosity measurements from LF-NMR (Fig. 11) support these findings. The control sample exhibits the highest porosity (~ 6.8%), while all LC^3 mixes show substantially lower values, with M20L15 achieving the lowest (~ 2.0%), consistent with its optimal pore structure. The reduction in total porosity is primarily attributed to the pore-filling effect of additional hydration products (C–A–S–H and carboaluminates) formed in LC^3 systems.

In summary, LF-NMR analysis demonstrates that LC^3 achieves a dual effect: it refines the pore size distribution by reducing capillary pores and lowers total porosity. This microstructural densification, combined with the chemical consumption of CH, effectively controls alkalinity leaching, enhancing the suitability of LC^3 for ecological concrete applications.

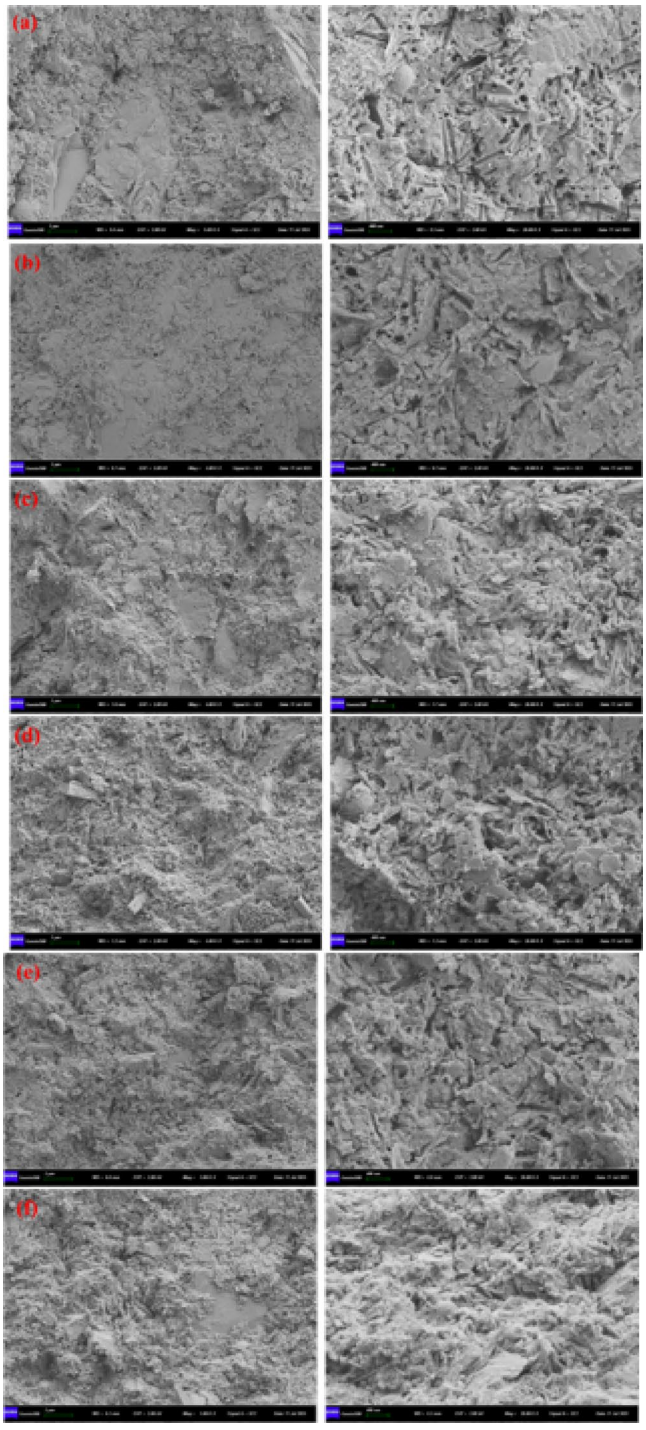

Fig. 9. SEM micrographs of LC^3 ecological concrete at 28 days: (**a**) ctrl; (**b**) M20L15; (**c**) M30L15; (**d**) M40L15; (**e**) M30L10; (f) M30L25.

Vegetative performance

Tall fescue was selected as the test plant species in this study. As a cool-season perennial grass, it is characterized by strong drought tolerance, adaptability to nutrient-poor conditions, and broad environmental resilience, and has therefore been widely employed in vegetated concrete systems and ecological slope protection projects[56,57]. In addition, tall fescue maintains relatively high germination rates and stable growth performance in the mildly alkaline environments typical of cement-based materials, making it a commonly adopted model species in studies of vegetated concrete. Owing to its proven engineering applicability and extensive research background, tall fescue was chosen as the representative plant for evaluating vegetation performance in this work[58].

The vegetative compatibility of LC^3 ecological concrete was assessed through the germination and growth of tall fescue (Festuca arundinacea), highlighting the critical roles of pore structure and chemical alkalinity.

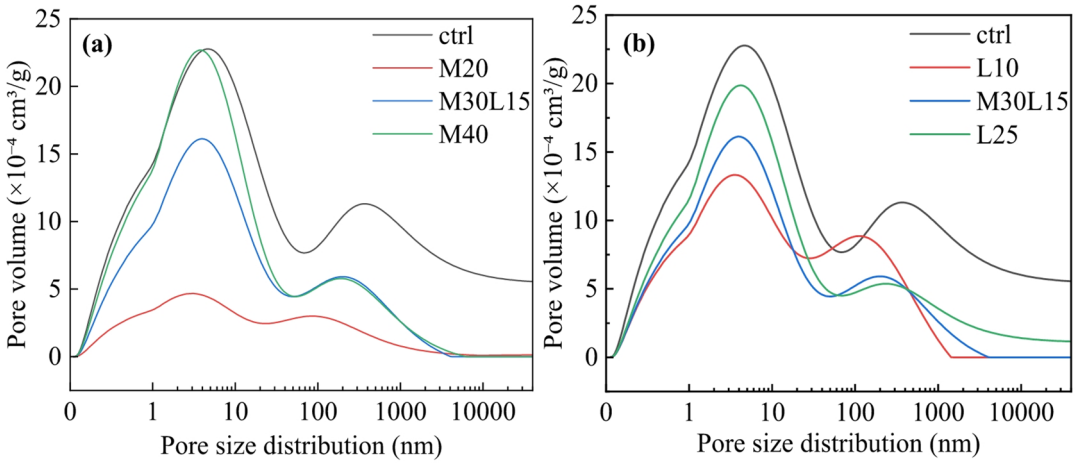

Fig. 10. Pore size distribution of LC^3 pastes measured by LF-NMR.

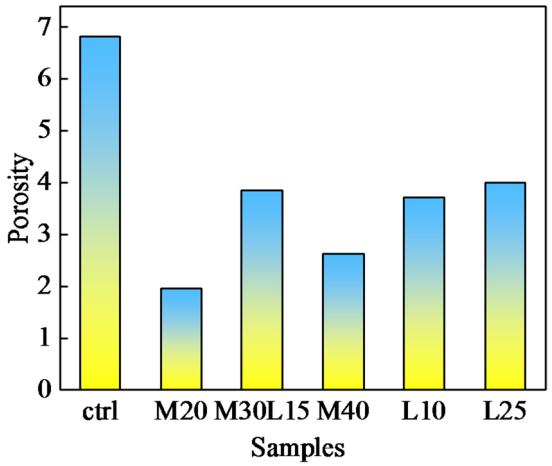

Fig. 11. Total porosity of LC^3 pastes determined by LF-NMR.

Figure 12 presents the germination time of tall fescue seeds. Seeds germinated earliest in specimens with 30% porosity, followed by 26%, while those with 22% porosity exhibited significant delays. This trend emphasizes the importance of porosity, as higher and well-connected pore volumes enhance water retention and oxygen diffusion, creating favorable conditions for seed imbibition and activation. Moreover, LC^3 mixtures with optimized compositions (e.g., M30L15 and M40L15) and lower alkalinity supported faster and more uniform germination compared to the high-alkalinity control group, indicating that both chemical and physical factors influence early plant establishment.

Tall fescue growth over 60 days is summarized in Fig. 13. The control group (100% OPC) initially germinated, but seedlings yellowed and withered around day 15, with complete mortality by day 20. This failure is attributed to sustained high alkalinity (pH > 12), which inhibits root development and nutrient uptake, combined with insufficient water retention. In contrast, all LC^3 mixtures supported healthy growth throughout the experimental period. Plants typically entered a rapid growth phase within 15–20 days, stabilizing at high shoot heights without decline. These results demonstrate that the reduced alkalinity and improved pore structure of LC^3 concrete provide a sustainable environment for vegetation.

Porosity had a pronounced effect on growth. At a constant mix composition, increasing porosity from 22% to 30% led to a marked increase in final plant height (e.g., from ~15 cm to over 20 cm at day 60), reflecting enhanced water and nutrient storage. When porosity was held constant, differences in growth among LC^3 mixes revealed the secondary, yet significant, influence of alkalinity. Mixes with the lowest pH (M30L15 and M40L15) consistently promoted superior growth across all porosity levels. The ongoing pozzolanic reactions in these systems consume $Ca(OH)_2$, lowering the pH to a plant-tolerable range (~8.5–9.0), closely mimicking natural soil conditions.

Figure 14 illustrates mid-to-late stage growth. LC^3-based concrete exhibited dense vegetation coverage and well-developed root systems penetrating the porous matrix. By contrast, the control group showed extensive bare areas due to root inhibition and plant mortality caused by high alkalinity.

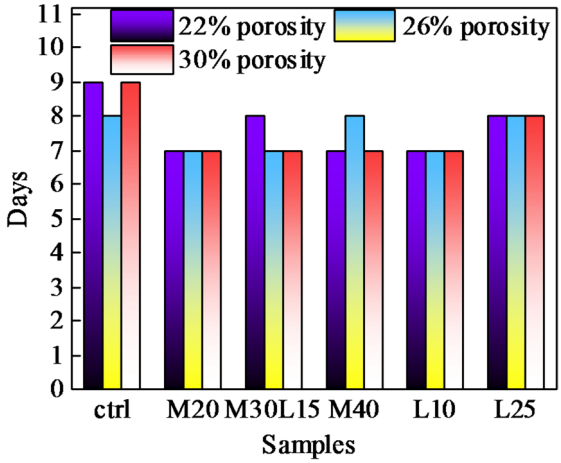

Fig. 12. Germination time of tall fescue in LC³ ecological concrete.

In summary, vegetative performance tests confirm that LC³ ecological concrete, particularly with porosity ≥ 25% and an optimized composition (e.g., M30L15), effectively balances mechanical integrity with ecological function. The synergistic combination of a plant-compatible alkaline environment and a supportive pore structure enables robust vegetation establishment and growth, demonstrating strong potential for applications in urban greening and slope stabilization.

Conclusion

This study systematically evaluated the application of Limestone Calcined Clay Cement (LC³) in ecological concrete, focusing on alkalinity control, mechanical performance, and vegetative compatibility. The key findings are summarized as follows:

(1) Incorporation of LC³ significantly enhances ecological concrete performance. It effectively reduces 28-day pH to a plant-compatible range (8.4–8.8) while maintaining high compressive strength. Mixes such as M20L15 and M30L15 achieved an optimal balance between low alkalinity and superior mechanical performance across different porosity levels. In addition, a low water-to-binder ratio (0.24) promotes a denser matrix, contributing to higher compressive strength (e.g., 13 MPa for M20L15) and more effective alkalinity suppression, particularly at lower porosities (22%).

(2) The observed reduction in alkalinity arises from a dual mechanism: (i) chemical consumption of portlandite (CH) via the pozzolanic reaction of metakaolin, and (ii) physical obstruction of ion transport through a refined pore network. The synergy between metakaolin and limestone facilitates the formation of C-A-S-H gels and carboaluminate phases, densifying the matrix. Microstructural analyses (XRD, TGA, SEM, LF-NMR) confirmed decreased CH content, increased carbonate phases, and pore refinement, collectively explaining the enhanced performance.

(3) Vegetation tests demonstrated the ecological benefits of LC³ concrete. An optimized pore structure (optimal porosity ~ 30%) ensured sufficient water retention and root penetration, while reduced alkalinity prevented the root inhibition observed in OPC specimens. Consequently, plants exhibited vigorous growth, with final heights exceeding 20 cm, confirming the material's suitability for ecological applications.

In conclusion, LC³ represents a highly promising, sustainable alternative to OPC for ecological concrete. By simultaneously optimizing chemical composition and pore structure, LC³ reconciles the often-conflicting demands of mechanical integrity and ecological function, making it a viable solution for applications such as slope stabilization and urban greening. This study provides a comprehensive framework for designing eco-friendly and resilient concrete materials.

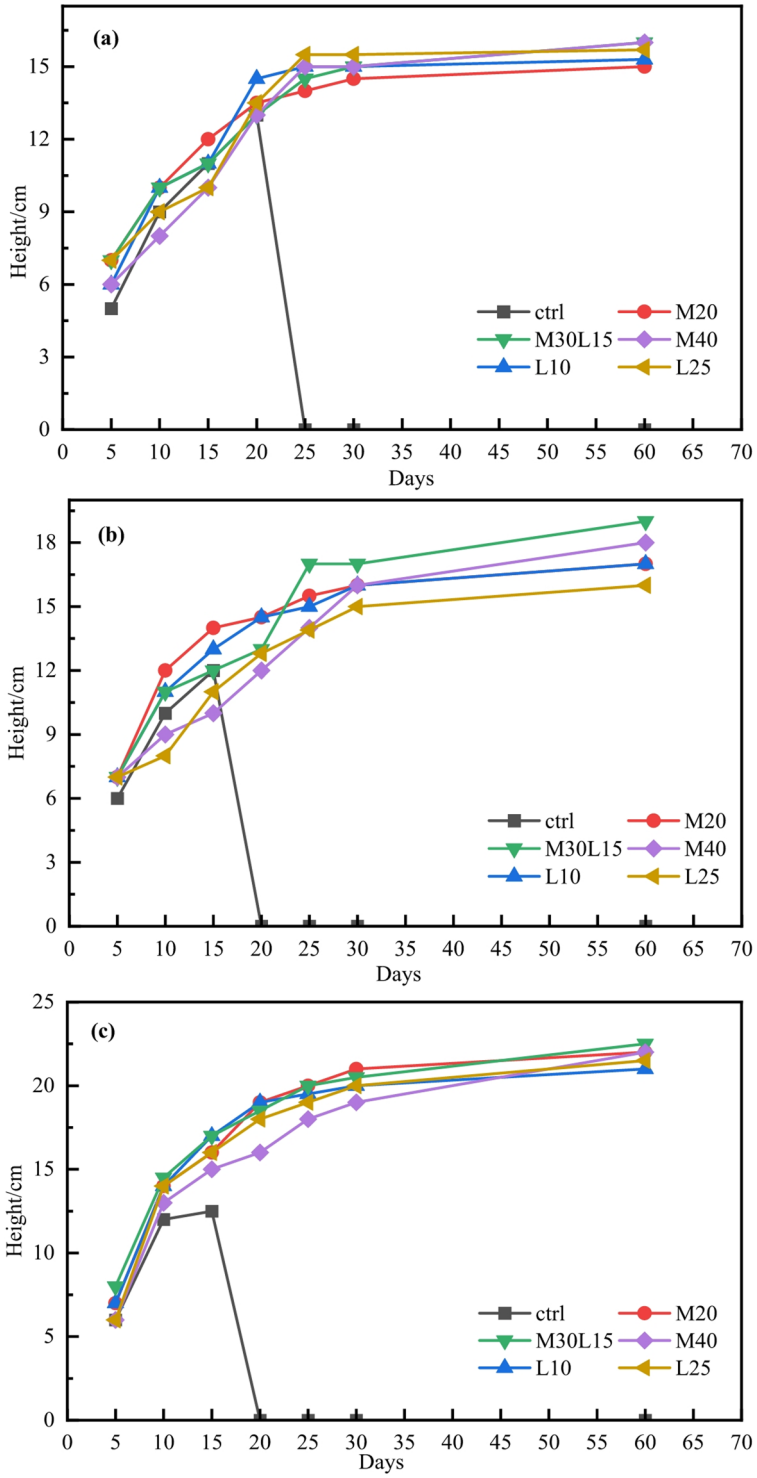

Fig. 13. Growth height of tall fescue in LC^3 ecological concrete at different porosities: (**a**) 22%; (**b**) 26%; (**c**) 30%.

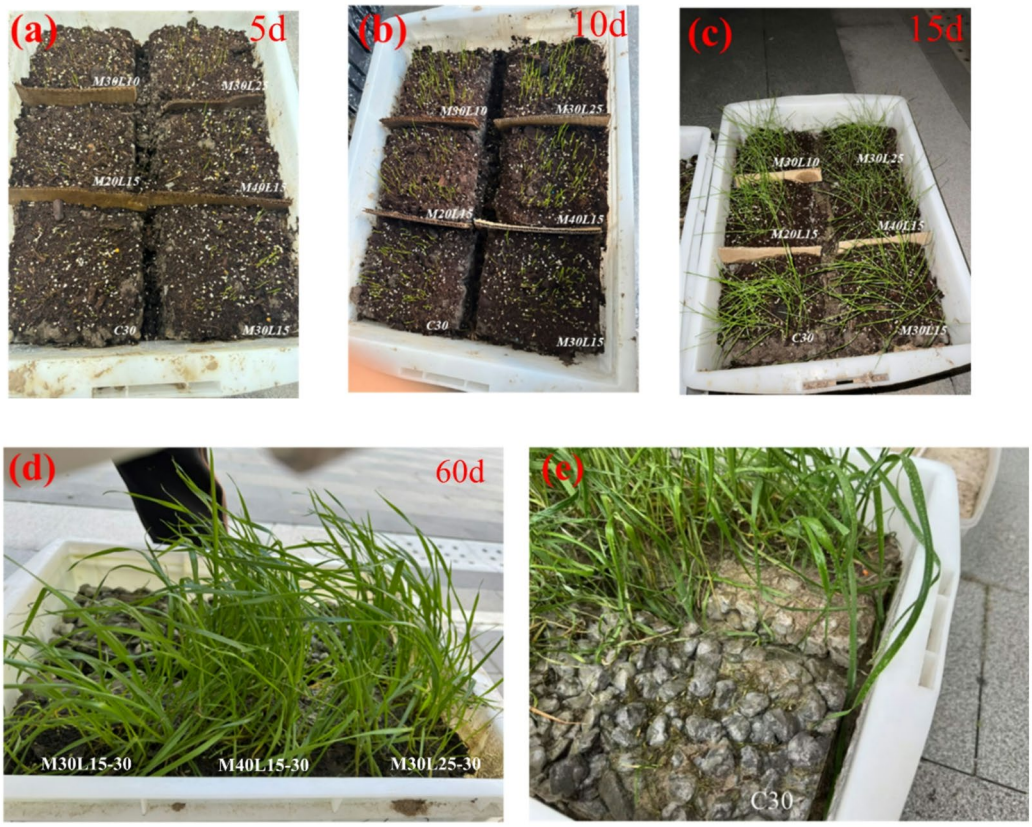

Fig. 14. Mid-to-late stage growth of vegetated concrete specimens.

Data availability

The data that support the findings of this study are available from the corresponding author upon reasonable request.

Received: 4 November 2025; Accepted: 29 January 2026
Published online: 02 February 2026

References

1. Zheng, C. et al. Review of porous vegetation eco-concrete (PVEC) technology: from engineering requirements to material design. *Compos. Part. B: Eng.* **279**, 111442 (2024).
2. Liu, C. et al. *Research and application progress of vegetation porous concrete. Mater. (Basel)* **16** (21). (2023).
3. Agrawal, R. et al. Urban Mining from biomass, brine, Sewage sludge, phosphogypsum and e-waste for reducing the environmental pollution: Current status of availability, potential, and technologies with a focus on LCA and TEA. **224** *Environ. Res.* (2023).
4. Gong, C. et al. Effects of carbamide on fluidity and setting time of sulphoaluminate cement and properties of planting concrete from sulphoaluminate cement. *Constr. Build. Mater.* **182**, 290–297 (2018).
5. Gong, C. C. et al. Effects of limestone powders on pore structure and physiological characteristics of planting concrete with sulfoaluminate cement. *Constr. Build. Mater.* **162**, 314–320 (2018).
6. Lyu, Q. et al. Plant-germination ability and mechanical strength of 3D printed vegetation concrete bound with cement and soil. *Constr. Build. Mater.* **408**, 133587 (2023).
7. Huang, J. et al. Study on corrosion characteristics of reinforcing bars in concrete under industrial SO2 environment. *Constr. Build. Mater.* **416**, 135177 (2024).
8. Li, S., Yin, J. & Zhang, G. Experimental investigation on optimization of vegetation performance of porous sea sand concrete mixtures by pH adjustment. *Constr. Build. Mater.* **249**, 118775 (2020).
9. Liu, Y. et al. State-of-the Art on preparation, performance, and ecological applications of planting concrete. *Case Stud. Constr. Mater.* **20**, e03131 (2024).
10. Ojo, M. et al. Electrochemical investigation of accelerated deterioration of concrete with iron-sulfide containing aggregates. *Cem. Concr. Res.* **182**, 107570 (2024).
11. Patrisia, Y. et al. Long-term durability of iron-rich geopolymer concrete in sulphate, acidic and peat environments. *J. Building Eng.* **97**, 110744 (2024).
12. Zhao, S. et al. Utilization of phosphogypsum and phosphate in improving water resistance of magnesium oxychloride cement. *Constr. Build. Mater.* **444**, 137777 (2024).
13. Ganapathy, G. P. et al. Effects of fly Ash and silica fume on alkalinity, strength and planting characteristics of vegetation porous concrete. *J. Mater. Res. Technol.* **24**, 5347–5360 (2023).
14. Huang, F. et al. A novel chitosan/biochar-modified eco-concrete with balanced mechanical, planting, and water purification performance for riparian restoration. *J. Clean. Prod.* **481**, 144144 (2024).
15. Lei, J. et al. Study on green restoration of exposed mountain: effect of isobutylidene diurea on slow-release of total nitrogen and physiological characteristics of euonymus fortune in planted eco-concrete. *Constr. Build. Mater.* **359**, 129460 (2022).

16. Zhang, X. et al. Research on physical properties and plant adaptability of polyurethane modified cement based planting concrete. *Constr. Build. Mater.* **466**, 140222 (2025).
17. Scrivener, K. et al. Calcined clay limestone cements (LC3). *Cem. Concr. Res.* **114**, 49–56 (2018).
18. Hay, R. & Celik, K. Effects of water-to-binder Ratios (w/b) and Superplasticizer on physicochemical, microstructural, and mechanical evolution of limestone calcined clay cement (LC3). *Constr. Build. Mater.* **391** (2023).
19. Lin, R. S. et al. Strengthening the performance of limestone-calcined clay cement (LC < SUP>3) using nano silica. *Constr. Build. Mater.* **340** (2022).
20. Wang, L. et al. On the use of limestone calcined clay cement (LC < SUP>3) in high-strength strain-hardening cement-based composites (HS-SHCC). *Cement Concrete Res. Constr. Build. Mater.* **144** (2021).
21. Wei, J. J. et al. Dynamical properties of environmental high-performance composites with calcined clay. *J. Clean Prod.* **335** (2022).
22. Zhang, D. et al. Engineered cementitious composites (ECC) with limestone calcined clay cement (LC < SUP>3). *Cement Concrete Composit.* **114** (2020).
23. Zunino, F. & Scrivener, K. The reaction between metakaolin and limestone and its effect in porosity refinement and mechanical properties *Cement Concrete Res.* **140** (2021).
24. El Mir, A. & Nehme, S. G. Effect of air entraining admixture on the properties of self-compacting concrete incorporating supplementary cementitious materials. *Pollack Periodica Pollack Periodica*. **12** (3), 85–98 (2017).
25. Mir, A. E. & Nehme, S. G. Porosity of Self-compacting concrete. *Procedia Eng.* **123**, 145–152 (2015).
26. Pillai, R. G. et al. Service life and life cycle assessment of reinforced concrete systems with limestone calcined clay cement (LC3). *Cement Concrete Res.* **118**, 111–119 (2019).
27. Pradhan, S., Poh, A. C. B. & Qian, S. Z. Impact of service life and system boundaries on life cycle assessment of sustainable concrete mixes. *J. Clean Prod.* 342 (2022).
28. Huang, X. et al. Performance assessment of LC3 concrete structures considering life-cycle cost and environmental impacts. *J. Clean. Prod.* **436**, 140380 (2024).
29. Akbulut, Z. F. et al. Exploring the flowability, physical, and mechanical properties of eco-friendly colored cement mortars with Metakaolin under sulfuric (H2SO4) and nitric acid (HNO3) attacks. *J. Building Eng.* **91**, 109463 (2024).
30. Jin, W. et al. Life cycle assessment of limestone calcined clay concrete: potential for low-carbon 3D printing. *Sustainable Mater. Technol.* **41**, e01119 (2024).
31. Niyomukiza, J. B., Eisazadeh, A. & Tangtermsirikul, S. Synergistic effect of calcined clay and fly Ash on the performance of porous vegetation concrete. *Constr. Build. Mater.* **458**, 139749 (2025).
32. Lothenbach, B., Scrivener, K. & Hooton, R. D. Supplementary cementitious materials. *Cem. Concr. Res.* **41** (12), 1244–1256 (2011).
33. Lin, R. S. et al. Strengthening the performance of limestone-calcined clay cement (LC3) using nano silica. *Constr. Build. Mater.* **340**, 127723 (2022).
34. Sun, J., Zunino, F. & Scrivener, K. Hydration and phase assemblage of limestone calcined clay cements (LC3) with clinker content below 50%. *Cem. Concr. Res.* **177**, 107417 (2024).
35. Chen, J. G. et al. Effect of aggregate size and water/cement on compressive strength and physiological performance of planting concrete. *Materials* **15** (19). (2022).
36. Yousuf, S. *Alkalinity of Cement Mortar Containing Different Types of Supplementary Cementitious Materials Under Accelerated Curing Conditions* (ProQuest LLC, 2021).
37. Muzenda, T. R. et al. The role of limestone and calcined clay on the rheological properties of LC3. *Cem. Concr. Compos.* **107**, 103516 (2020).
38. Li, Q. & Fan, Y. Rheological evaluation of nano-metakaolin cement pastes based on the water film thickness. *Constr. Build. Mater.* **324**, 126517 (2022).
39. Kim, H. H. & Park, C. G. Plant growth and water purification of porous vegetation concrete formed of blast furnace Slag, natural jute fiber and styrene butadiene latex. *Sustainability* **8** https://doi.org/10.3390/su8040386 (2016).
40. Zhuang, P. et al. Study on the performance optimization of Plant-Growing ecological concrete. *Sustainability* **16** https://doi.org/10.3390/su16114575 (2024).
41. Zunino, F. & Scrivener, K. Hydration and strength development of low-clinker (< 50%) factor limestone calcined clay cements (LC3): A comparative study with natural Pozzolans. *Constr. Build. Mater.* **499**, 144075 (2025).
42. Avet, F. & Scrivener, K. Influence of pH on the chloride binding capacity of limestone calcined clay cements (LC < SUP>3). *Cement Concrete Res.* **131**. (2020).
43. Canbek, O., Washburn, N. R. & Kurtis, K. E. Relating LC < SUP>3 microstructure, surface resistivity and compressive strength development. *Cement Concrete Res.* **160** (2022).
44. Gong, C. et al. Effects of limestone powders on pore structure and physiological characteristics of planting concrete with sulfoaluminate cement. *Constr. Build. Mater.* **162**, 314–320 (2018).
45. Krishnan, S. & Bishnoi, S. A Numerical approach for designing composite cements with calcined clay and limestone. *Constr. Build. Mater.* **138** (2020).
46. Wang, Y. et al. Corrosion mechanism of reinforcement in LC3 cement pastes under coupled carbonation and chloride attack. *Cem. Concr. Compos.* **140**, 105080 (2023).
47. Hay, R. & Celik, K. Effects of water-to-binder ratios (w/b) and superplasticizer on physicochemical, microstructural, and mechanical evolution of limestone calcined clay cement (LC3). *Construct. Build. Mater.* **391**, 131529. (2023).
48. Karkhaneh, S., Tarighat, A., Ghaffarpour, S. & Jahromi Kinetics behavior of delayed ettringite in limestone calcined clay cement (LC3) by thermodynamic approach and consideration of the time factor. *Constr. Build. Mater.* **367**, 129143 (2023).
49. Huang, Z., Liang, T. & Chen, L. Experimental studies on durability performances of ultra-lightweight low-carbon LC3 cement composites against chloride ingression and carbonation. *Constr. Build. Mater.* **395**, 132340 (2023).
50. Liu, M. et al. Effects of colloidal nanoSiO2 on the hydration and hardening properties of limestone calcined clay cement (LC3). *Constr. Build. Mater.* **411**, 134371 (2024).
51. Wu, F., Chen, X. & Brouwers, H. J. H. Application of miscanthus to enhance plant growth adaptability of bio-based vegetal concrete. *Constr. Build. Mater.* **425**, 136096 (2024).
52. Gong, X. et al. Characterisation and application of plant growth under stress of Grass-planting concrete with alkaline variations. *Case Stud. Constr. Mater.* **22**, e04517 (2025).
53. Pritzl, M. D., Tabatabai, H. & Ghorbanpoor, A. Long-term chloride profiles in Bridge decks treated with penetrating sealer or corrosion inhibitors. *Constr. Build. Mater.* **101**, 1037–1046 (2015).
54. Wang, X. et al. Material characterization to assess effectiveness of surface treatment to prevent joint deterioration from oxychloride formation mechanism. *Cem. Concr. Compos.* **104**, 103394 (2019).
55. Martínez, A. & Miller, S. A. Life cycle assessment and production cost of geopolymer concrete: A meta-analysis. *Resour. Conserv. Recycl.* **215**, 108018 (2025).
56. Guo, W., Zhang, W. & Han, L. Effects of Water–Nitrogen interaction on sandy soil, physiology, and morphology of tall fescue (Festuca arundinacea Schreb) turf. *Agriculture* **14** https://doi.org/10.3390/agriculture14111948 (2024).
57. Liu, C. et al. Research and application progress of vegetation porous concrete. *Materials* **16** https://doi.org/10.3390/ma16217039 (2023).
58. Chen, J. et al. Effect of aggregate size and Water/Cement on compressive strength and physiological performance of planting concrete. *Materials* **15**, 6685. https://doi.org/10.3390/ma15196685 (2022).

Author contributions

Yi Fang : Conceptualization, Funding acquisition, Writing-reviewing and editing. **Cheng Yang** : Methodology, Investigation, Visualization, Writing—original draft. **Hui Zeng: ** Investigation. **Jin Yang: ** Investigation. **Hailong Zhang: ** Investigation. **Yue Gu: ** Investigation. **Hongqiang Chu** : Investigation, Supervision. **Linhua Jiang** : Investigation.

Funding

This work is supported by the Fundamental Research Funds for the Central Universities at Hohai University, Natural Science Foundation of Jiangsu Province (BK20241525), and National Natural Science Foundation of China (52508263).

Declarations

Competing interests

The authors declare no competing interests.

Additional information

Correspondence and requests for materials should be addressed to Y.F. or H.C.

Reprints and permissions information is available at www.nature.com/reprints.

Publisher's note Springer Nature remains neutral with regard to jurisdictional claims in published maps and institutional affiliations.